

Space charge *distribution* measurement methods and particle loaded insulating materials

S. Holé¹, A. Sylvestre², O. Gallot Lavallée³, C. Guillermin⁴, P. Rain² and S. Rowe⁴

¹Laboratoire des Instruments et Systèmes d'Ile de France

Université Pierre et Marie Curie-Paris6 - 10, rue Vauquelin, 75005 Paris - France

²Laboratoire d'Électrostatique et des Matériaux Diélectriques

CNRS UMR5517 - 25, avenue des Martyrs, BP 166, 38042 Grenoble cedex 9 - France

³Laboratoire d'Étude Aérodynamiques

CNRS UMR6609 - boulevard Marie & Pierre Curie, Téléport 2

BP 30179, 86962 Futuroscope, Chasseneuil, France

⁴Schneider Electric Industries S.A.S. - 22, rue Henry Tarze 38000 Grenoble - France

6th January 2006

Abstract

In this paper the authors discuss the effects of particles (fillers) mixed in a composite polymer on the space charge measurement techniques. The origin of particle-induced spurious signals is determined and silica filled epoxy resin is analysed by using the laser-induced-pressure-pulse (LIPP), the pulsed-electro-acoustic (PEA) and the laser-induced-thermal-pulse (LITP) methods. A spurious signal identified as the consequence of a piezoelectric effect of some silica particles is visible for all the methods. Moreover, space charges are clearly detected at the epoxy/silica interface after a 10-kV/mm poling at room temperature for 2 hours.

1 Introduction

Large breakdown value is not the ultimate insulating material characteristic sought for by these days. For example a large strength can be necessary for the material to resist mechanical stresses, or a higher conductivity above a given electric field threshold can be necessary to prevent damage due to breakdown. In order to reach such complex material characteristics, additive particles are often introduced in a host material [1, 2, 3]. The material overall cost is also an important parameter for industrial applications which can be greatly reduced by the addition of low cost filler particles to a relatively high cost host material.

The addition of particles for improving one physical or commercial characteristic can however be detrimental to another one. In the case of electrical insulation, particles can lead to charge buildup and then to accelerated aging. They can also increase the electrical conductivity and then reduce the material electrical strength.

Space charge measurement methods, such as the pressure-wave-propagation method, the thermal method, or the electro-acoustic method, give access in a non-destructive way to the distribution of space charges in an insulating material [4]. These three measurement methods are based either on thermal diffusion or elastic wave propagation, and electrostatics. In the case of the thermal or the pressure-wave-propagation methods, the diffusion of heat or the propagation of an elastic wave through the material to be tested generates an electrical response directly correlated with the space charge distribution in the material. In the case of the electro-acoustic method, a rapid variation of the electric field in the material to be tested produces elastic waves which profile is directly correlated with the space charge distribution in the material. These elastic waves are measured by an adjacent transducer. The correspondence between the space charge distribution and the measured signal depends on the electrical, mechanical and thermal properties of the material to be tested. When the material is uniform, its properties do not vary in space and the correspondence between the space charge and the signal is constant during a measurement. Conversely when the material includes particles, its properties vary in space and therefore the correspondence between the space charge and the signal changes during the measurement. This results in particle-induced proportional perturbation. Furthermore particles may also be polarized or present piezoelectric properties independently to the space charge in the material. This results in a particle induced additional perturbation. As a consequence the signal obtained from particle loaded materials must be analyzed carefully as to avoid mis-interpretation due to the various particle-induced signal perturbations (spurious signals) [5].

In this paper we first recall the origin of the signal induced by the implementation of the various space charge distribution measurement methods. Then particle-induced signal perturbations are identified and analyzed depending on particle thermal, mechanical and electrical properties, on particle granulometry, and on particle distribution throughout the host material. Experimental results are shown with silica loaded Epoxy resin and the laser-induced-thermal-pulse (LITP), the laser-induced-pressure-pulse (LIPP), and pulsed-electro-acoustic (PEA) methods.

2 Physical background

The presence of particles in the material can alter space charge measurements in two ways: firstly by perturbing the diffusion of heat or the propagation of pressure waves, and secondly by adding spurious signals. These different alterations are studied in the following subsections.

2.1 Heat diffusion and elastic wave propagation

The thermal methods rely on thermal diffusion to perform space charge measurements, and the pressure-wave-propagation and the electro-acoustic methods rely on wave propagation. Any perturbation to the diffusion of heat or to the propagation of pressure waves may therefore alter these measurement methods.

The equation of heat diffusion depends on the mass density m_v , the heat capacity per mass unit c , the thermal conductivity λ , and the temperature increase from the equilibrium ΔT as

$$m_v c \frac{\partial \Delta T}{\partial t} = \text{div}(\lambda \vec{g} \text{rad}(\Delta T)). \quad (1)$$

Similarly the equation of propagation depends on the mass density m_v , the elastic stiffness coefficient C , and the material displacement \vec{u} as

$$m_v \frac{\partial^2 \vec{u}}{\partial t^2} = \vec{g} \text{rad}(C \text{div}(\vec{u})). \quad (2)$$

Equations (1) and (2) impose temperature ΔT , heat flux $\lambda \vec{g} \text{rad}(\Delta T)$, displacement \vec{u} , and stress $C \text{div}(\vec{u})$ to be continuous at any position in space. As a consequence, the spatial discontinuities of the material properties, specially at the interfaces host material-particles, make an incident heat diffusion or wave propagation to partially reflect and transmit as illustrated in Figure 1a. Figure 1b shows the decomposition of the incident, reflected and transmitted stress or temperature profiles through an interface in normal incidence. As expected, the sum of these profiles (Figure 1c) is continuous. In normal incidence the reflexion coefficient $\gamma_{1 \rightarrow 2}$ and the transmission coefficient $\tau_{1 \rightarrow 2}$ for the heat flux or the stress from a medium 1 to a medium 2 are

$$\gamma_{1 \rightarrow 2} = \frac{Z_2 - Z_1}{Z_2 + Z_1} \quad (3)$$

$$\tau_{1 \rightarrow 2} = \frac{2Z_2}{Z_2 + Z_1} \quad (4)$$

where Z is the material impedance. In the case of heat diffusion the thermal impedance, also known as effusivity, is $Z = \sqrt{m_v c \lambda}$ [6]. In the case of elastic wave propagation the acoustic impedance is $Z = \sqrt{m_v C}$ [7].

Particles are however more closely shaped as spheres than as planes. Therefore reflexions and transmissions scatter in all directions and attenuate in amplitude as the square of the distance from the particle. In addition, the larger the particle diameter, the larger the amplitude of the scattered reflections and transmissions. This is simulated in two-dimensions in Figure 2 for diffusion, and in Figure 3 for propagation. In these simulations, the particle impedance is 3 times the one of the host material. In Figure 2a and 2b the temperature profile is almost unaltered by small particles but clearly deformed by larger particles. In Figure 3a and 3b the wave front is also almost unaltered by small particles (top) whereas it is almost cut by larger particles (bottom). *The radius of particles is generally compared with the wavelength of a propagating wave [7]. The radius of a large particle is larger than the wavelength whereas the radius of a small particle is smaller than the wavelength. In the case of transient diffusion of propagation however, the smallest significant wavelength λ_m has to be taken into account in order to characterize the size of a particle. Typically λ_m is twice the extent at mid-amplitude of a pulse or twice the distance from 10% to 90% of a step amplitude.* In other words *particle diameter* is small or large in comparison with the spatial resolution of the measurement method. *For an elastic wave propagation it ranges from 5 to 100 μm and for heat diffusion it is linearly dependent on the depth, being 5 μm at 5- μm depth and 100 μm at 100- μm depth.* In Figures 2c, 2d, 3c and 3d, the incident diffusion or propagation has been removed in order to observe in a better way the reflection and transmission. One can notice that, as expected, the scattered reflexion and transmission are larger and act at longer distance for the large particle.

When more particles are taken into account, reflections and transmissions from each particle sum up over *a volume which thickness is the resolution and section is the surface of the heat or the elastic wave front*. Since particles are randomly positioned in the host material and since many particles are laterally involved during the measurement, the local reflections and transmissions statistically compensate except on the axis of the incident diffusion or propagation. Therefore the overall direction of the diffusion or the propagation remains unaffected and the equivalent properties of the material layer is an average of the properties of particles and the host material as shown in Figure 4. As a consequence, when the lateral extent is much larger than *resolution*, a one dimensional model is still correct insofar as one introduces a spatial dependence for the material properties in order to take into account the slight variations of equivalent properties between the material layers. *Of course, as in the case of conventional planar samples, the incident heat diffusion and elastic wave propagation are assumed planar, and the electrodes parallel.*

The mean distance between particles and the mean particle size perturb differently the incident diffusion or propagation depending on the measurement resolution, that is to say the distance over which the temperature or the pressure profile mainly varies.

If the particle diameter is smaller than the resolution then reflections and transmissions from particles are small and act at short distances (see top of Figures 2 and 3). The temperature or pressure profile is attenuated and dispersed with time but keeps a similar shape, for instance a pulse remains a pulse. Examples are shown in Figure 5a and 5b with 5- μm -diameter alumina particles and 50- μm -diameter silica particles in Epoxy resin. In that case the mean distance between particles affects only the speed at which attenuation and dispersion occur. Such a degradation can be compensated by using the usual deconvolution algorithms [8, 9, 10, 11] and appropriate determination of the material properties [12].

If the particle diameter is larger than the resolution then reflections and transmissions from particles are large and act at long distances (see bottom of Figures 2 and 3). In the case of a mean distance between particles smaller than the resolution, the temperature or the pressure profile is altered by small and rapid perturbations which may induce small oscillations in the signal. An example is shown in Figure 5c with 200- μm -diameter niobate lithium particles in the same Epoxy resin. Since the induced oscillations are only due to the particle distribution and not to the space charge distribution, a low-pass filter might be used before applying the deconvolution usual algorithms [8, 9, 10, 11, 12]. As the mean distance between particles increase as compared to the resolution, oscillations in the signal become larger and last a longer time. The original thermal or pressure profile becomes completely altered and it is necessary to apply a lower pass-filter or an envelope detection algorithm in order to remove the alterations before the deconvolution algorithms. The resolution is then very reduced. This latter situation is fortunately not often encountered.

2.2 Measured signal and particle induced perturbations

It has been shown that one-dimensional model can be applied to particle filled material insofar as many particles are involved laterally and as material property variations are allowed between sample layers. When the sample is uniform, the correspondence (gain) between the space charge and the signal, which depends on the material properties, is identical *at any position in the sample* during the measurement. This correspondence can be determined once by a calibration measurement. However when the sample includes particles, the material properties vary from one position to the other and the correspondence (gain) between the space charge and the signal varies *in the sample* during the measurement. *A given charge density at*

a given position in the sample may therefore produce a different signal amplitude than the same charge density at another position. As a consequence the particles induce a perturbation proportional to the space-charge-induced signal, hereafter denoted as particle-induced proportional perturbation.

Particles may also present a net charge, a dipolar orientation or be made of piezoelectric material for instance. They can therefore generate their proper signal in addition to the one generated by the space charges in the sample. As a consequence particles can also induce an additive perturbation, hereafter denoted as particle-induced additional perturbation.

The proportional and the additional perturbations can be estimated by the signal expression of the different measurement methods.

For the thermal or the pressure wave propagation methods [13], the measured current i_m for a planar sample of thickness d is

$$i_m = -C_0 \frac{\partial}{\partial t} \int_0^d [(1 - a/\epsilon)E + (\pi - e)/\epsilon] \frac{\partial u}{\partial z} dz, \quad (5)$$

where the material deformation $\partial u/\partial z$ is equal to $\alpha\Delta T$ in the case of the thermal methods, α being the expansion coefficient, and to $-\chi P$ in the case of the pressure-wave-propagation method, χ being the material compressibility and P the pressure. C_0 is the capacity of the sample at rest, ϵ is the permittivity, a is the electrostrictive coefficient, E is the electric field, π is the permanently oriented dipole density, and e is the piezoelectric coefficient.

For the electro-acoustic method [13], the deformation $\partial u/\partial z$ at the transducer position z_t is

$$\begin{aligned} \frac{\partial u}{\partial z} = & -C_0 \int_0^d \int_{t'}^d [(1 - a/\epsilon)E + (\pi - e)/\epsilon] V(t') G(z_t, z, t - t') dt' dz \\ & + \frac{C_0^2}{2A^2} \int_0^d \int_{t'}^d \frac{\epsilon - a}{\epsilon^2} V^2(t') G(z_t, z, t - t') dt' dz \end{aligned} \quad (6)$$

where G is the Green's function, V is the voltage pulse applied for the measurement, and A is the stressed area. The green's function indicates how an elastic wave is modified from its source to the position z_t where it is measured. For non-lossy materials one has

$$G = \frac{\chi}{2} \frac{\partial}{\partial z} \delta(t - t' - (z - z_t)/v_s) \quad (7)$$

where δ is the Dirac's function and v_s is the speed of sound.

In the case of particles present a net charge or a permanent dipolar orientation, they generate an electric field which superimposes to the one generated by the space charge and the applied voltage. The electric field E in (5) and (6) is then the sum of the electric field E_p generated by space charge and the applied voltage, and of the electric field E' generated by particles.

The signal generated by the space charge distribution and the applied voltage through E_p is proportional to $\alpha(1 - a/\epsilon)$ or $\chi(1 - a/\epsilon)$. Therefore the spatial variations of a , ϵ , α and χ produce a particle-induced proportional perturbation.

The signal generated by particles through E' , π and e appears in addition. Therefore E' , π and e produce a particle-induced additional perturbation. Since this perturbation does not depend on space charge distribution or the applied voltage, it can be measured once under short-circuit when the sample is still virgin (free

of charge). However the random distribution of particles makes the additional perturbation to be highly related to the location of the measurement. Therefore the sample cannot be removed, even temporarily, from its holder unless it is strictly repositioned identically. Figure 6 shows additional perturbations measured at different lateral locations on an Epoxy resin sample containing silica fillers with the thermal and the pressure-wave-propagation methods. Very different responses are obtained in the regions including particles even for lateral displacements as small as a quarter of the lateral extent, about 2 mm.

3 Experimental validation

The different behaviors theoretically predicted in the former section are shown experimentally in this section using the thermal pulse, pressure-wave-propagation and electro-acoustic methods. For this purpose test samples were made in Epoxy resin including 50- μm -diameter silica particles as shown in Figure 7. It has been previously reported [5, 14] that a fraction of these particles exhibit a piezoelectric behavior. Particles being produced from natural river sand, some of them has the α -quartz crystalline structure which is a well known piezoelectric material.

In order to emphasize additive and proportional perturbations, samples contain two 500- μm -thick regions, one particle free and the other particle filled as illustrated in Figure 7b. For thermal pulse method however a 150- μm -thick sample with an homogeneous particle distribution was made in order to improve the signal to noise ratio (Figure 7c).

Laser-induced-pressure-pulse (LIPP) measurements under short-circuit, -2 kV and -3 kV applied voltages are shown in Figure 8. It can be noticed that under short-circuit (Figure 8a) a signal is visible only when the pressure pulse is in the particle filled region of the sample. This cannot be due to charges or dipoles trapped in particles since in that case an interfacial peak should have been detected owing to the electric field generated by the charges or dipoles. This can be due to piezoelectricity however, since in that case an electric response is generated only when particles are mechanically stressed, that is to say when the pressure reaches the particles. Under voltage (Figure 8b), the particle-induced spurious signals are clearly visible between the two interfacial peaks due to induced charges on the sample electrodes. They are not strictly similar to the one under short-circuit due to a superimposed proportional perturbation. That proportional particle-induced perturbation can be isolated by subtracting from under-voltage measurements the one made under short-circuit to remove the additive perturbation. The normalisation with the applied voltage shows now very similar profiles in Figure 8c. This is mainly due to the variation in permittivity between the two regions of the sample (peak) and to the slight variation of permittivity within the particle filled region.

Pulsed-electro-acoustic (PEA) measurements under short-circuit, -2 kV and -3 kV applied voltages are shown in Figure 9. As in the case of the LIPP method, a signal is detected under short circuit (Figure 9a) only in the region of particles. A small signal is however detected at the front electrode but is due to the term in V^2 in the signal (Equation (6)). By subtracting this signal from those under voltage (Figure 9b) in order to remove the additive perturbation and by normalising with applied voltage, one obtains similar results for both applied voltages due to the proportional perturbation induced by the permittivity spatial variations (Figure 9c).

Laser-induced-thermal-pulse (LITP) measurements under short-circuit, +200 V and +300 V applied voltages are shown in Figure 10. In this sample particles are uniformly distributed. The spurious signal is thus present even at time 0. Under short-circuit (Figure 10a), the signal is only due to the piezoelectric particles. By subtracting the short-circuit measurement from those under voltage (Figure 10b) in order to remove the additional perturbation, and by normalising with applied voltages, one obtains similar signal (Figure 10c). The remaining small oscillations are due to the spatial variation of permittivity.

Finally additional and proportional perturbations have been observed for all kind of measurement methods. It can be noticed that the proportional perturbation is smaller in uniformly filled region than at the interface between two regions with different particle distributions (Figure 8c and 9c). Indeed, the variation of permittivity between layers is smaller in uniformly filled materials than between unfilled and filled materials.

4 Study of an industrial silica filler Epoxy sample

Epoxy resin used in this study is a DGEBA type resin, cured with an acid anhydride. Silica fillers are mixed with the epoxy (60% of fillers in weight). The glass transition temperature T_g of the polymer is about 65 °C. Two sample geometries are used as illustrated in Figure 11. The first geometry consists in 1-mm-thick discs of filled Epoxy resin with 2 aluminium electrodes deposited by radio-frequency sputtering. The second geometry consists in massive aluminium electrodes molded in the Epoxy resin during curing. The sample thickness is 0.5 mm in this latter case.

The tail of silica fillers is non-uniform and their particle diameter ranges from 1 μm to 100 μm (Figure 7a). The larger population of particles is around 50 μm diameter. These silica fillers are produced from natural crushed river sand so some of them show piezoelectric properties (α -quartz crystalline structure).

The LIPP method is used hereafter to investigate space charges in these samples. The reader can refer to [14] for PEA measurements on similar samples.

4.1 Effect of piezoelectricity on the space charge measurement

LIPP signals obtained in short-circuit condition for two silica filled Epoxy resins (roller wheels) subjected to 40 °C and 80 °C respectively, are shown in Figure 12. *They have been calibrated separately in order to take into account the variation of sound velocity with temperature [15].* An internal signal is clearly detectable and shows oscillations which frequency is strongly correlated with the mean particle diameter. It cannot be attributed to space charges since it is not modified after a cure at 120 °C for two weeks under short-circuit. It can be attributed however to the piezoelectricity of SiO_2 filler particles [5, 14]. Indeed α -quartz, which is a well known piezoelectric material, is a possible crystalline structure for some of the particles.

Measurements for both samples in Figure 12 are very different and temperature cannot explain this difference. In fact, as piezoelectric fillers are oriented at random in the Epoxy matrix, only particles at the position of the pressure pulse are taken into account in the resulting signal. Two different samples exhibit therefore two different signals. The signal damping for position greater than 0.25 mm in the case of 40 °C

and 0.15 mm in the case of 80 °C can be attributed to attenuation and dispersion of the pressure pulse during its propagation. Indeed, as the pressure extent increases, more particles are mechanically stressed producing in turn more signal sources and thus more statistical compensation. Since dispersion and attenuation increase with temperature, the damping is more important at 80 °C than at 40 °C.

4.2 Influence of silica fillers on the pressure pulse propagation

Independently to the piezoelectric effect, it is important to analyse the influence of SiO₂ particles on the pressure pulse propagation. Measurements *at room temperature* of 1-mm-thick Epoxy resin discs with or without silica fillers are presented in Figure 13. A 10-kV stress is applied to the back electrode of the samples for the measurements.

It can be firstly observed that the sound velocity is 20 % greater for the silica filled Epoxy resin. This result suggests that the pressure wave goes through silica particles instead of passing round them. A sound velocity around 2500 m/s is measured for the Epoxy matrix against 3000 m/s for the silica filled Epoxy matrix.

It can be secondly observed that the pressure pulse attenuates 50 % more in the silica filled Epoxy sample, in spite of a larger velocity. This confirms non-negligible reflections at the Epoxy/silica filler interfaces, which disperse the energy of pressure pulse. Since the peaks at both electrode interfaces do not show superimposed oscillations, it can be concluded that particles affect only the speed at which attenuation and dispersion occur as discussed in section 2.1.

4.3 Space charges detection

A silica filled Epoxy resin sample has been subjected to 10 kV/mm for 2 hours *at room temperature*. Measurements are reported in Figure 14 at the beginning (black curve) and at the end (gray curve) of the stress cycle. The interfacial peak increase after 2 hours poling indicates a global polarization. Within the sample, oscillations are clearly increased compared to the signal just after applied the voltage. Unambiguously, space charges are trapped at the Epoxy/silica interfaces.

5 Conclusion

In this paper we have analyzed the implications of filler particles on different space charge measurement techniques. Particles may produce proportional or additional perturbations to the space charge distribution signal independently to the measurement method being implemented. A silica filled Epoxy resin sample has been used as an illustration. Silica particles exhibiting piezoelectricity, they induce a random like signal during the measurement owing to the random distribution and orientation of the particle in the host material. Knowing the effect of particles on the signal we have concluded that the evolution of the signal after a voltage stress is due to charge trapping around particles.

References

- [1] C.P. Wong and R.S. Bollampally. Thermal conductivity, elastic modulus, and coefficient of thermal expansion of polymer composites filled with ceramic particles for electronic packaging. *J. Appl. Polym. Sci.*, 74:3396–3403, 1999.
- [2] KP Donnelly and BR Varlow. Non-linear dc and ac conductivity in electrically insulating composites. *IEEE Trans. Dielectr. EI.*, 10:610–614, 2003.
- [3] M Harada, M Morimoto, and M Ochi. Influence of network chain orientation on the mechanical property of epoxy resin filled with silica particles. *J. Appl. Polym. Sci.*, 87:787–794, 2003.
- [4] T. Mizutani. Space charge techniques and space charge in polyethylene. *IEEE Trans. Dielectr. EI.*, 1:923–933, 1994.
- [5] S. Holé, A. Sylvestre, and S. Rowe. The influence of filler particles on space charge measurements. *J. Phys. D: Appl. Phys.*, 37:1869–1876, 2004.
- [6] D.P. Almond and P.M. Patel. *Photothermal science and techniques*. Chapman & Hall, UK, 1996. ISBN: 0412578808.
- [7] P. M. Morse and K. U. Ingard. *Theoretical acoustics*. McGraw-Hill Inc, New York, U.S.A., 1968. ASIN: 070433305.
- [8] D.L. Phillips. A technique for the numerical solution of certain integral equations of the first kind. *J. ACM*, 9:84–97, 1962.
- [9] S. Twomey. On the numerical solution of fredholm integral equations of the first kind by the inversion of the linear system produced by quadrature. *J. ACM*, 10:97–101, 1963.
- [10] P. Bloß, R. Emmerich, and Bauer S. Thermal wave probing of pyroelectric distributions in the surface region of ferroelectric materials: a new method for the analysis. *J. Appl. Phys.*, 72:5363–5370, 1992.
- [11] S.B. Lang. Laser intensity modulation method (LIMM): experimental techniques, theory and solution of integral equation. *Ferroelectrics*, 118:343–361, 1991.
- [12] T. Ditchi, C. Alquié, and J. Lewiner. Broadband determination of ultrasonic attenuation and phase velocity in insulating materials. *J. Acoust. Soc. Am.*, 94:3061–3066, 1993.
- [13] S. Holé, T. Ditchi, and J. Lewiner. Non-destructive methods for space charge distribution measurements: what are the differences? *IEEE Trans. Dielectr. EI.*, 10:670–677, 2003.
- [14] O. Gallot-Lavallee, G. Teyssedre, C. Laurent, and S. Rowe. Space charge behaviour in an epoxy resin: the influence of fillers, temperature and electrode material. *J. Phys. D: Appl. Phys.*, 38:2017–2025, 2005.
- [15] K.R. Bambery and R.J. Fleming. The temperature dependence of space charge accumulation in cross-linked polyethylene. *J. Therm. Anal.*, 50:19–31, 1997.

Figure Captions

Figure 1: Example of temperature and stress profiles due to partial reflection and transmission. (a) directions. (b) incident, reflected and transmitted parts. The dotted lines represent the continuation of the profiles as if there were no interfaces. (c) complete profile, *i.e.* sum of incident, reflected and transmitted parts.

Figure 2: Reflection and transmission of an incident plane diffusion on a small diameter particle (top) or on a larger diameter particle (bottom). The particle has an effusivity 3 times the one of the host material. (a) complete temperature profile at the particle. (b) complete temperature profile after the particle. (c) only reflection and transmission at the particle. (d) only reflection and transmission after the particle. The scales represent the normalised temperature increase amplitude.

Figure 3: Reflection and transmission of an incident plane wave on a small diameter particle (top) or on a larger diameter particle (bottom). The particle has an impedance 3 times the one of the host material. (a) complete stress profile at the particle. (b) complete stress profile after the particle. (c) only reflection and transmission at the particle. (d) only reflection and transmission after the particle. The scale represents the normalised stress amplitude.

Figure 4: Equivalent parameters. (a) reflections and transmissions from each particles. (b) overall reflections and transmissions from a particle layer. (c) equivalent parameters of the particle layer.

Figure 5: Pulse degradation due to particles. (a) 5- μm -diameter Al_2O_3 particles, (b) 50- μm -diameter SiO_2 particles and (c) 200- μm -diameter LiNbO_3 particles.

Figure 6: Measurement lateral position dependence. (a) pressure-wave-propagation method and (b) thermal pulse method.

Figure 7: Epoxy silica compound for experimental validation. (a) silica particle micro-photograph 300 μm \times 400 μm . (b) sample for the pressure-wave-propagation and electro-acoustic methods. (c) sample for thermal-pulse method.

Figure 8: Measurements with the laser-induced-pressure-pulse (LIPP) method. (a) under short circuit, (b) under voltage, and (c) normalised after subtraction of the additive perturbation (short-circuit signal)

Figure 9: Measurements with the pulsed-electro-acoustic (PEA) method. (a) under short circuit, (b) under voltage, and (c) normalised after subtraction of the additive perturbation (short-circuit signal).

Figure 10: Measurements with the laser-induced-thermal-pulse (LITP) method. (a) under short circuit, (b) under voltage, and (c) normalised after subtraction of the additive perturbation (short-circuit signal).

Figure 11: Sample geometries: (a) disc, and (b) *roller wheel*.

Figure 12: Short-circuit measurements at 40 °C and 80 °C in silica filled Epoxy resin. (one specific sample for each temperature)

Figure 13: LIPP response in a 1-mm thick Epoxy resin sample subjected to 10 kV applied on the back electrode.

Figure 14: 1-mm thick silica filled Epoxy resin sample subjected to 10 kV/mm for 2 hours.

Figure 1 - S. Holé, A. Sylvestre, O. Gallot Lavallée, C. Guillermin, P. Rain and S. Rowe

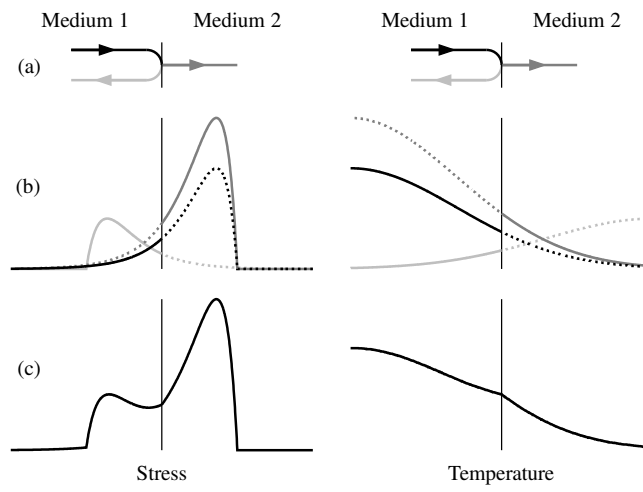


Figure 2 - S. Holé, A. Sylvestre, O. Gallot Lavallée, C. Guillermin, P. Rain and S. Rowe

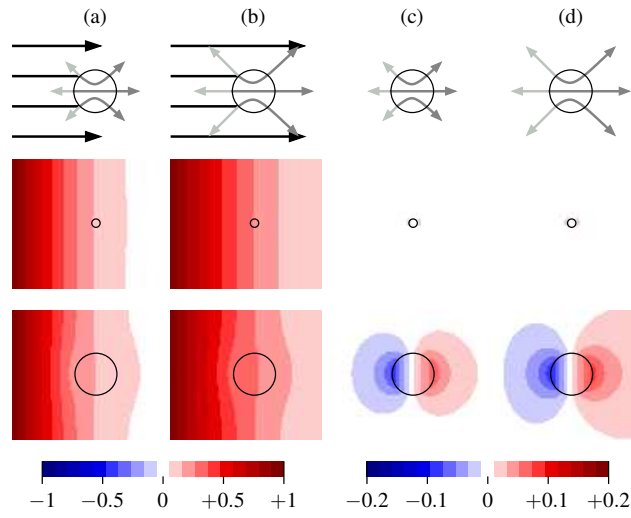


Figure 3 - S. Holé, A. Sylvestre, O. Gallot Lavallée, C. Guillermin, P. Rain and S. Rowe

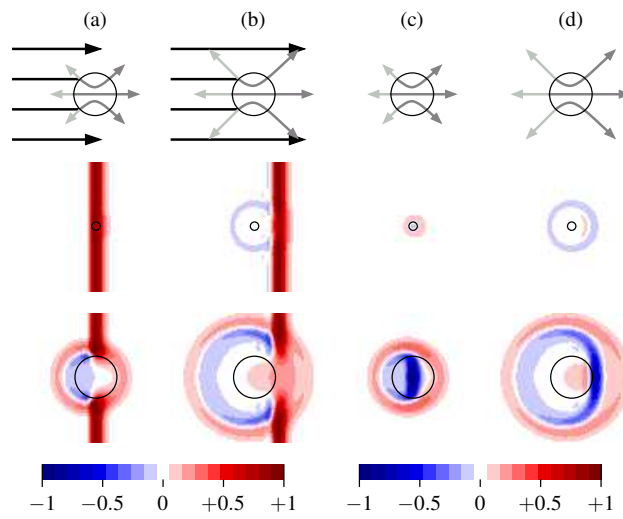


Figure 4 - S. Holé, A. Sylvestre, O. Gallot Lavallée, C. Guillermin, P. Rain and S. Rowe

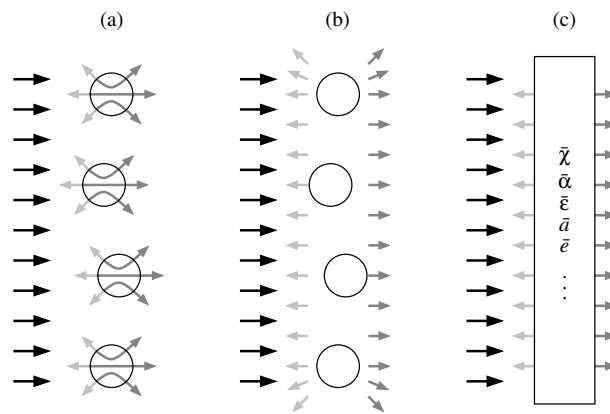


Figure 5 - S. Holé, A. Sylvestre, O. Gallot Lavallée, C. Guillermin, P. Rain and S. Rowe

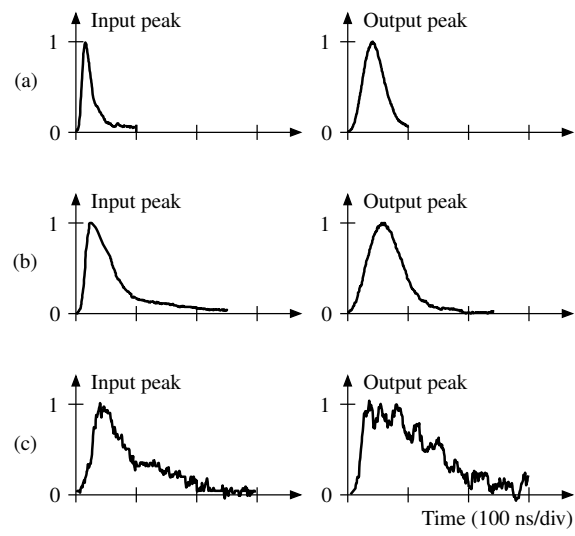


Figure 6 - S. Holé, A. Sylvestre, O. Gallot Lavallée, C. Guillermin, P. Rain and S. Rowe

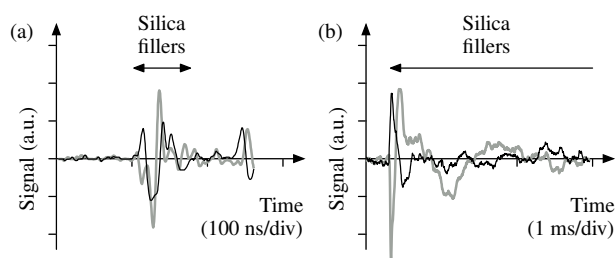


Figure 7 - S. Holé, A. Sylvestre, O. Gallot Lavallée, C. Guillermin, P. Rain and S. Rowe

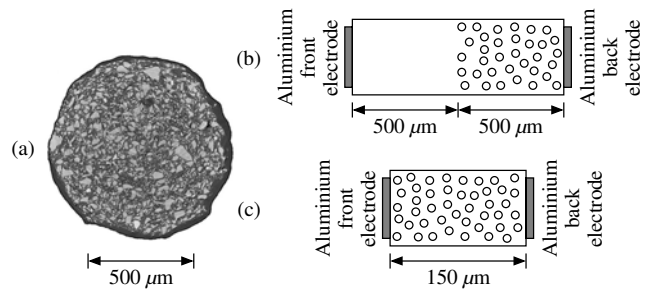


Figure 8 - S. Holé, A. Sylvestre, O. Gallot Lavallée, C. Guillermin, P. Rain and S. Rowe

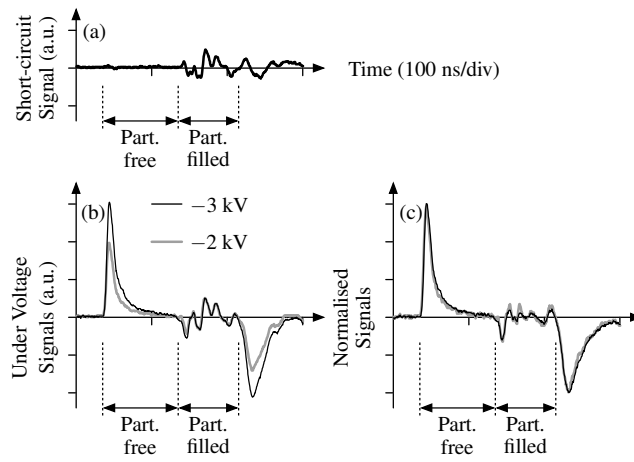


Figure 9 - S. Holé, A. Sylvestre, O. Gallot Lavallée, C. Guillermin, P. Rain and S. Rowe

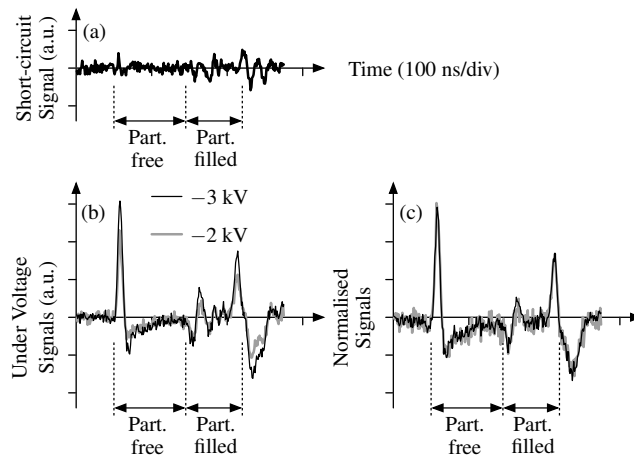


Figure 10 - S. Holé, A. Sylvestre, O. Gallot Lavallée, C. Guillermin, P. Rain and S. Rowe

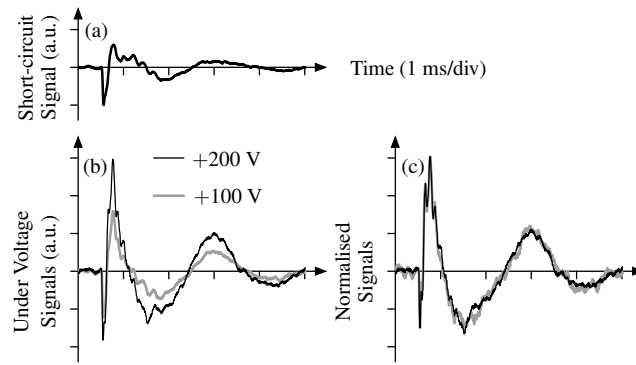


Figure 11 - S. Holé, A. Sylvestre, O. Gallot Lavallée, C. Guillermin, P. Rain and S. Rowe

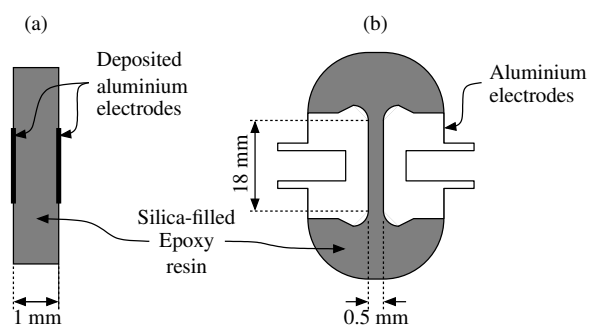


Figure 12 - S. Holé, A. Sylvestre, O. Gallot Lavallée, C. Guillermin, P. Rain and S. Rowe

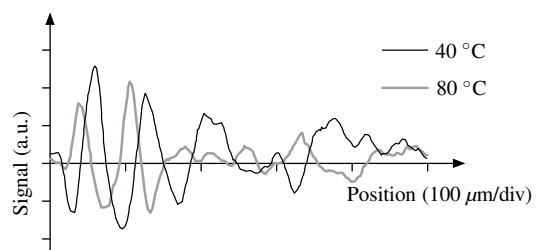


Figure 13 - S. Holé, A. Sylvestre, O. Gallot Lavallée, C. Guillermin, P. Rain and S. Rowe

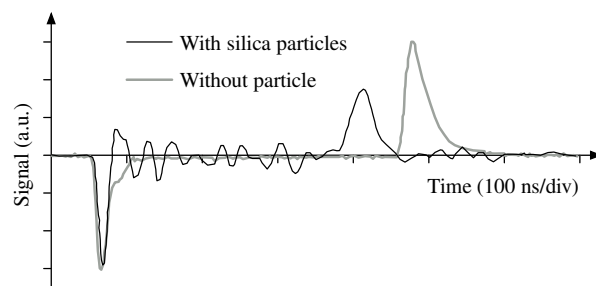


Figure 14 - S. Holé, A. Sylvestre, O. Gallot Lavallée, C. Guillermin, P. Rain and S. Rowe

